Kybernetika

Junxiao Wang; Fengxiang Wang; Xianbo Wang; Li Yu

Disturbance observer based integral terminal sliding mode control for permanent magnet synchronous motor system

Kybernetika, Vol. 55 (2019), No. 3, 586–603

Persistent URL: `http://dml.cz/dmlcz/147864`

KYBERNETIKA — VOLUME *55* (2019), NUMBER 3, PAGES 586–603

DISTURBANCE OBSERVER BASED INTEGRAL TERMINAL SLIDING MODE CONTROL FOR PERMANENT MAGNET SYNCHRONOUS MOTOR SYSTEM

Junxiao Wang, Fengxiang Wang, Xianbo Wang and Li Yu

This paper presents speed regulation issue of Permanent Magnet Synchronous Motor (PMSM) using a composite integral terminal sliding mode control scheme via a disturbance compensation technique. The PMSM q-axis and d-axis subsystems are firstly transformed into two linear subsystems by using feedback linearization technique, then, integral terminal sliding mode controller and finite-time controller are designed respectively. The proof of finite time stability are given for the PMSM closed-loop system. Compared with the corresponding asymptotical stability control method, the proposed controller can make the system output track the desired speed reference signal in finite time and obtain a better dynamic response and anti-disturbance performance. Meanwhile, considering the large chattering phenomenon caused by high switching gains, a composite integral terminal sliding mode control method based on disturbance observer is proposed to reduce chattering phenomenon. Through disturbance estimation based feed-forward compensation, the composite integral terminal sliding mode controller may take a smaller value for the switching gain without sacrificing disturbance rejection performance. Experimental results are provided to show the superiority of proposed control method.

Keywords: PMSM, integral terminal sliding mode control, finite-time control, feedback linearization, disturbance observer

Classification: 93C73, 93C95

1. INTRODUCTION

Permanent magnet synchronous motor (PMSM) system has been widely employed in industry applications due to its high performance such as compact structure, high air-gap flux density, high power density, high torque to inertia ratio, and high efficiency [26]. However, PMSM control system is essentially a nonlinear system with unknown load torque disturbances, friction and unmodel dynamics [31]. It is not easy to achieve a satisfactory high performance when using traditional control methods. Hence, many advanced control methods could become a consideration to improve performance of PMSM system [33].

DOI: 10.14736/kyb-2019-3-0586

To enhance the speed regulation performance, many advanced control methods have been developed for the PMSM system, such as input-output linearization control [34], adaptive control [19], robust control [11], back-stepping control [28, 35], fractional order control [24], disturbance estimation based control [10, 32, 33], neural network control [29], fuzzy control [14], etc. These advanced control methods are used for improving system performance from different aspects.

Recently, more and more researchers take interest on finite-time control issues, not only because of the faster convergence rate around the equilibrium, but also for the fact that such systems seem to perform better disturbance rejection abilities [9, 2]. The finite-time control systems is of great significance because finite-time convergence have some nice features such as better dynamic response and disturbance rejection properties [20]. In addition, considering the traditional sliding mode methods which employ linear sliding surfaces can only ensure the system state in infinite time [13, 17, 22], for accelerating the rate of convergence, the terminal sliding mode method which adopts nonlinear sliding surfaces is proposed. The nonsingular terminal sliding mode method can ensure convergence of the system state in finite time. The nonsingular terminal sliding mode methods are given by [7] which are regarded to be efficient methods to improve the system disturbance rejection properties [23], but the switching gain also cause large chattering phenomenon.

For dealing with the disturbance problems for PMSM control system, disturbances reject methods have been proposed. An extended state observer (ESO) is employed to estimate the lump disturbances of PMSM system in [20, 22], it regards the lumped disturbances, which consist of a friction force, torque ripple, unmodelled dynamics and load variation. In [20], a finite-time controller plus feed-forward compensation based on ESO can improve the disturbance rejection property. The proper switching gain of sliding mode controller only need to be taken bigger than the bound of disturbance compensation error for reducing chattering after feed forward compensation for these disturbances in [22, 23]. A fuzzy sliding mode control method is proposed for the speed control problem of PMSM system, where a simple load torque observer method is used to estimate the disturbance for tuning the switching gain [16]. The paper [18] introduces a radial basis function network (RBFN) disturbance observer design method which also can estimate the lumped PMSM disturbances and improve the system robustness.

In this paper, we propose a q-axis second order speed control law and a d-axis current controller for improving the tracking performance and disturbance rejection capabilities for PMSM servo system. Different from the above algorithms, firstly, the approach in this paper are finite-time control and integral terminal sliding mode control which is produced by combining integral sliding mode method and finite-time control theory [36]. What is more, for the speed-regulation problem, traditional speed loop control design is usually a first-order model for approximately describing the relationship between the reference q-axis current and the speed loop output, so the reference q-axis current i_q^* is regarded the same as the q-axis current i_q. Considering the speed loop control period and the current loop control period are becoming smaller or even vanishing. In this case, neglecting the current dynamics will degrade the closed loop performance of PMSM system. We adopt a second-order model of speed loop which is built for describing the relationship between the reference q-axis current and the speed output of PMSM system [23]. Moreover, considering the nature chattering problem of sliding mode control method, to estimate the lump disturbance for reducing chattering of PMSM system, a feed-forward compensation term based on disturbance observation (DOB) for the lumped disturbances of system is added to integral terminal sliding mode (ITSM) feedback term. The disturbances are estimated by using disturbance observer (DOB) which can obtain better closed-loop performance [5, 8]. This feed-forward compensation design helps to select a smaller switching gain for integral terminal sliding mode controller which can reduce chattering. Comparative studies are also carried out by simulations and experiments.

The remainder of this paper is organized as follows. In Section II, the mathematical model of PMSM and some theorems of finite-time control are described. In Section III, the q-axis and d-axis controller design and stability analysis based on integral terminal sliding mode control and finite time control are presented in details, the experimental results are given. In Section IV, a chattering attenuation method using DOB technique is also described, experiment results are also discussed in this part. Finally, a conclusion ends this paper.

2. MATHEMATICAL MODEL OF PMSM AND PRELIMINARIES

2.1. Mathematical model of PMSM

The surface-mounted PMSM is considered in this paper, suppose that magnetic circuit is unsaturated, hysteresis and eddy current loss are ignored and the magnetic field in the air gap has a sinusoidal distribution along the circumference. In the $d-q$ coordinates, the ideal mathematical model of the surface mounted PMSM is expressed as follows [26]:

$$\dot{\omega} = \frac{k_t i_q}{J} - \frac{B\omega}{J} - \frac{T_l}{J} \tag{1}$$

$$\dot{i}_q = -\frac{R_s i_q}{L_q} + n_p \omega i_d - \frac{n_p \psi \omega}{L_q} + \frac{u_q}{L_q} \tag{2}$$

$$\dot{i}_d = -\frac{R_s i_d}{L_d} + n_p \omega i_q + \frac{u_d}{L_d} \tag{3}$$

where R_s the stator resistance, u_d, u_q the input voltages, i_d, i_q the d-axis and q-axis stator currents, L_d, L_q the d-axis and q-axis stator inductances, with $L_d = L_q = L_s$, n_p the number of pole pairs of the PMSM, ω the rotor angular velocity of the motor, ψ the flux linkage, T_l the load torque, B the viscous friction coefficient, J the rotor inertia, $k_t = \frac{1.5 n_p \psi_f}{J}$ the torque constant, and ψ_f the flux linkage. From Eqs. (2) – (3), we know that currents of i_d and i_q are coupled. From Eqs. (1) – (3), we also could know that the relative degree of ω and u_q for q-axis subsystem is second order, the relative degree of i_d and u_d for d-axis subsystem is first order.

The output of PMSM servo system is the speed ω. For the control design of speed loop, the motor speed dynamic equation (1) could be rewritten as

$$\dot{\omega} = b i_q^* + d_0(t) \tag{4}$$

where $b = \frac{k_t}{J}$, $d_0(t) = \frac{k_t(i_q^* - i_q)}{J} - \frac{B\omega}{J} - \frac{T_l}{J}$ is regarded as the system disturbances including friction, load disturbances and tracking error of i_q current loop. This approximation may degrade the closed loop performance of PMSM. In [23], a second-order model between reference q-axis current and speed output is proposed, the form is

$$\ddot{\omega} = -\frac{k_i}{k_p}\dot{\omega} - \frac{B}{J}\dot{\omega} - \frac{Bk_i}{Jk_p}\omega - \frac{\dot{T}_l}{J} - \frac{T_l k_i}{Jk_p} - \frac{b}{k_p}\dot{u}_q + b\Big(\dot{i}_q^* + \frac{k_i}{k_p} i_q^*\Big) \quad (5)$$

where k_p and k_i are parameter values of PI controller for inner current loop, then Eq. 5 could be simplified as

$$\ddot{\omega} = u + d(t) \quad (6)$$

where $u = b(\dot{i}_q^* + \frac{k_i}{k_p} i_q^*)$, $d(t) = -\frac{k_i}{k_p}\dot{\omega} - \frac{B}{J}\dot{\omega} - \frac{Bk_i}{Jk_p}\omega - \frac{\dot{T}_l}{J} - \frac{T_l k_i}{Jk_p} - \frac{b}{k_p}\dot{u}_q$ can be considered as the lumped disturbance, u is the control signal.

2.2. Preliminaries

Lemma 2.1 (Bhat and Bernstein [1]): Consider a nonlinear system described by

$$\dot{x} = f(x), f(0) = 0, x \in R^n \quad (7)$$

Suppose that there exists a continuous function $V(x)$: $U \to R$ such that:

1. $V(x)$ is positive definite.
2. There exists real numbers $c > 0$ and $\alpha \in (0,1)$ and an open neighborhood $U_0 \subset U$ of the origin such that $\dot{V} \leq -cV^{\alpha}(x), x \in U_0$. Then, the origin is a finite-time stable equilibrium of system.

Lemma 2.2 (Bhat and Bernstein [2]): Consider a first order system.

$$\dot{x} = u \quad (8)$$

x and u are the state and control law. If the control law is selected as

$$u = -ksig^{\alpha}(x) \quad (9)$$

$k > 0, 0 < \alpha < 1, sig^{\alpha}(x) = sign(x)|x|^{\alpha}$. Then the system is globally finite-time stable.

Lemma 2.3 (Bhat and Bernstein [3]): Consider the integral chain system

$$\dot{x}_1 = x_2, \dot{x}_2 = u. \quad (10)$$

The origin is a globally finite-time stable equilibrium for the integral system under the feedback law

$$u = -k_1 sig^{\alpha_1}(x_1) - k_2 sig^{\alpha_2}(x_2) \quad (11)$$

where $k_1, k_2 > 0$, and α_1, α_2 satisfy $\alpha_2 = \frac{2\alpha_1}{1+\alpha_1}$ with $0 < \alpha_1 < 1$.

3. CONTROLLER DESIGN

For improving the servo performance of PMSM system, integral terminal sliding mode controller and finite-time controller are designed respectively for the q-axis subsystem and the d-axis subsystem. The general control structure of the PMSM servo system is shown as Figure 1, the overall system consists of a PMSM, space vector pulse width modulation (SVPWM), a voltage-source inverter (VSI), a field-orientation mechanism and three controllers. Here speed controller which is based on feedback-linearization technique is used to stabilize errors of q-axis speed, finite-time controller is adopted in the d-axis current loops which can stabilize d-axis current errors. As it can be seen from Figure 1, the rotor angle and velocity information can be obtained from the measurements. The currents i_d and i_q can be calculated from i_a, i_b and i_c (which could be obtained from measurements) by Clarke and Park transformations.

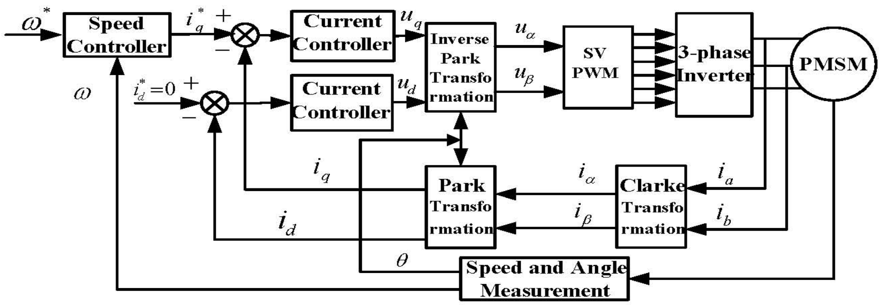

Fig. 1. Block diagram of PMSM servo system based on vector control.

3.1. Design of q-axis speed controller based on integral terminal sliding mode control method

The objective of this section is to design a q-axis integral terminal sliding mode controller as Figure 2 based on feedback-linearization, make the output of system track the reference speed signal in finite-time.

The reference speed value ω^* can be differentiable for the second order. Define the error of speed $e_\omega = \omega^* - \omega$, using the PMSM mathematical model of Eqs. (1) – (3), it yields

$$\begin{aligned} \dot{e}_\omega &= \dot{\omega}^* - \dot{\omega} \\ &= \dot{\omega}^* - \frac{3n_p\psi_f i_q}{2J} + \frac{B\omega}{J} + \frac{T_l}{J} \qquad (12) \\ \ddot{e}_\omega &= \ddot{\omega}^* - u - d(t) \qquad (13) \end{aligned}$$

Where $d(t) = -\frac{k_i}{k_p}\dot{\omega} - \frac{B}{J}\dot{\omega} - \frac{Bk_i}{Jk_p}\omega - \frac{\dot{T}_l}{J} - \frac{T_l k_i}{Jk_p} - \frac{b}{k_p}\dot{u}_q$. Define $x_1 = e_\omega, x_2 = \dot{e}_\omega$, thus,

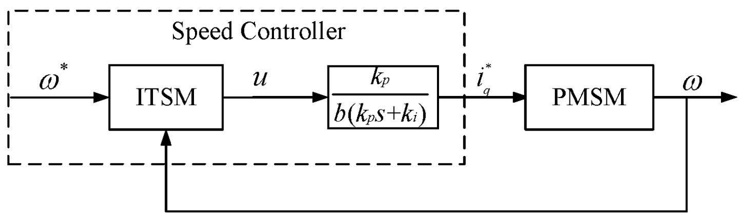

Fig. 2. Block diagram of PMSM servo system based on ITSM control.

the system could be simplified as:

$$\dot{x}_1 = x_2 \tag{14}$$
$$\dot{x}_2 = -u - d(t) + \ddot{\omega}^* \tag{15}$$

Eqs. (14) − (15) is a second order system.

Design an integral terminal sliding mode (ITSM) surface as,

$$s = x_2(t) - x_2(t_0) + \int_{t_0}^{t} (k_1 sig^{\alpha_1}(x_1(t)) + k_2 sig^{\alpha_2}(x_2(t)))\,\mathrm{d}t \tag{16}$$

where $k_1, k_2 > 0$,and α_1, α_2 satisfy $\alpha_2 = \frac{2\alpha_1}{1+\alpha_1}$ with $0 < \alpha_1 < 1$. Note that it is $s(t_0) = 0$ at $t = t_0$, so sliding mode stage starts from the initial time instance.

The control law is

$$u = k_1 sig^{\alpha_1}(x_1(t)) + k_2 sig^{\alpha_2}(x_2(t)) + \eta sgn(s) + \ddot{\omega}^* \tag{17}$$

from Eq. (6), it could obtain

$$b\Big(\dot{i}_q^* + \frac{k_i}{k_p} i_q^*\Big) = k_1 sig^{\alpha_1}(x_1(t)) + k_2 sig^{\alpha_2}(x_2(t)) + \eta sgn(s) + \ddot{\omega}^* \tag{18}$$

where $\eta > l$, $k_1, k_2 > 0$, and α_1, α_2 satisfy $\alpha_2 = \frac{2\alpha_1}{1+\alpha_1}$ with $0 < \alpha_1 < 1$.

3.2. Design of d-axis current controller based on finite time control method

The objective of this section is to design a d-axis current controller based on finite-time control and feedback-linearization technology, the reference $i_d^* = 0$, the output of controller is u_d. On the basis of PMSM mathematical model, define the error of d-axis current $e_d = i_d^* - i_d$. The equation of error state is

$$\dot{e}_d = -\dot{i}_d = \frac{R_s i_d}{L} - n_p \omega i_q - \frac{u_d}{L} \tag{19}$$

Define

$$u_1 = -\dot{i}_d = \frac{R_s i_d}{L} - n_p \omega i_q - \frac{u_d}{L} \tag{20}$$

then, the first order system is

$$\dot{e}_d = u_1 \tag{21}$$

the control law is

$$u_1 = -ksig^{\alpha}(e_d) \tag{22}$$

where $k > 0, 0 < \alpha < 1$.

The d-axis control voltage of u_d is deduced from Eqs. (20), (22), substituting the e_d with $-i_d$, yields

$$u_d = L\left(\frac{R_s i_d}{L} - n_p \omega i_q - ksig^{\alpha}(i_d)\right) \tag{23}$$

where $k > 0, 0 < \alpha < 1$.

3.3. Closed-loop stability

The closed-loop system stability analysis here consists of the analysis for q-axis subsystem which adopts integral terminal sliding mode (ITSM) controller and d-axis subsystem which adopts finite-time controller (FTC).

Assumption 3.1: For the PMSM servo system, suppose the lump disturbance $d(t)$ is bounded and satisfieslim$_{t\to\infty} \dot{d}(t) = 0$, suppose there exists a constant $l > 0$, and it satisfies $|d(t)| \leq l$.

Theorem 3.1: Suppose the PMSM servo system satisfies Assumption 3.1, the i_q^* and i_d^* control laws are designed as above Eq. (18) and Eq. (23) , if the switching gain satisfies $\eta > l$, then the closed-loop speed servo system of Eqs. (1) – (3), (18) and (23) is globally finite-time stable.

Proof. For the standard second integrator chain system of Eqs. (14) – (15), choosing the following Lyapunov function

$$V = \frac{1}{2} s^T s. \tag{24}$$

By taking the time derivative of V by using above Eq. (17), we obtain

$$\dot{V} = s\dot{s} = s(\dot{x}_2 + k_1 sig^{\alpha_1}(x_1) + k_2 sig^{\alpha_2}(x_2)) \tag{25}$$

substituting Eq. (17) into Eq. (15), yields

$$\begin{aligned} \dot{x}_2 &= -u_1 - d(t) = -k_1 sig^{\alpha_1}(x_1) - k_2 sig^{\alpha_2}(x_2) \\ &- \eta sgn(s) - d(t) \end{aligned} \tag{26}$$

substituting Eq. (26) into Eq. (25), yields

$$\begin{aligned}\dot{V} &= s(-\eta sgn(s) - d(t)) \leq\mid s \mid (-\eta + l) \\ &= 2^{\frac{1}{2}}(-\eta + l)\left(\frac{1}{2}s^T s\right)^{\frac{1}{2}} = -2^{\frac{1}{2}}(\eta - l)V^{\frac{1}{2}}. \end{aligned} \tag{27}$$

The Eq. (27) satisfies Lemma 2.1, so the system state is stabilized to sliding mode surface in finite-time t_{q1} when $\eta > l \geq |d(t)|$.

From the above analysis, the system states could reach the sliding surface $s = 0$ from any initial condition in finite-time t_{q1}, then $\dot{s} = 0$, yields

$$\dot{s} = \dot{x}_2 + k_1 sig^{\alpha_1}(x_1) + k_2 sig^{\alpha_2}(x_2) = 0 \tag{28}$$

According to Lemma 2.3, we know that the system state can converge to the origin along the sliding surface in finite-time t_{q2} . This completes the proof of q-axis closed-loop subsystem stability.

Substituting the d-axis subsystem with the u_d control law Eq. (23), then the closed-loop subsystem of d-axis current is

$$\dot{i}_d = -ksig^{\alpha}(i_d) \tag{29}$$

According to Lemma 2.2, the above d-axis current closed-loop subsystem is globally finite-time stable, i_d converges to the origin in a finite-time t_d. This completes the proof. □

Remark 3.1: When $\alpha = 1$, $\alpha_1 = 1$ and $\alpha_2 = 1$, Eq. (18) and Eq.(23) reduce to the following asymptotically stable controller (ASC) form.

$$b(\dot{i}_q^* + \frac{k_i}{k_p} i^*{}_q) = k_1 sig(x_1(t)) + k_2 sig(x_2(t)) + \eta sgn(s) + \ddot{\omega}^* \tag{30}$$

$$u_d = L\left(\frac{R_s i_d}{L} - n_p \omega i_q - k i_d\right) \tag{31}$$

where $\eta > l \geq |d(t)|$, $k, k_1, k_2 > 0$.

3.4. Experimental results

The parameters of the PMSM are given as Table 1, these parameter value are given by manufacturer and experimental test. This comparison for these two control schemes of ITSM control method and ASC method are implemented using DSP2808 based test bench as Figure 3.

The experiment parameter is selected as following Table 2. Figure 4(a) and Figure 4(c) show that the speed response and current response based on ITSM control method and FTC give a shorter settling time compared with ASC method. When in the presence of disturbance from Figure 5(a), Figure 5(c), and Figure 5(e), the ITSM control method and finite control method have less speed fluctuation (speed drop of ASC method has 67 rpm, but the ITSM has about 45 rpm.) and a shorter settling time compared with the ASC control method. i_q^* and u_d also recover faster than that of ASC from Figure 4(b), Figure 4(d), Figure 5(b), Figure 5(d), and Figure 5(f).

Descriptions	Parameters	Nominal Values
Rated Power	P	$750W$
Rated Voltage	U	$200\ V$
Number of Poles	n_p	4
Armature Resistance	Rs	$1.74,\ \Omega$
Stator Inductances	$L_d = L_q$	$0.004H,$
Viscous Damping	B	$7.403{\times}10^{-5}N \cdot m \cdot s/rad$
Momentum of Inertia	J	$1.78\ {\times}10^{-4}kg \cdot m^2$
Rated Speed	n	$3000\ RPM$
Rotor Flux Linkage	φ	$0.1167\ Wb$
rated torque	T_N	$2.0\ N \cdot m$

Tab. 1. Parameter values of PMSM.

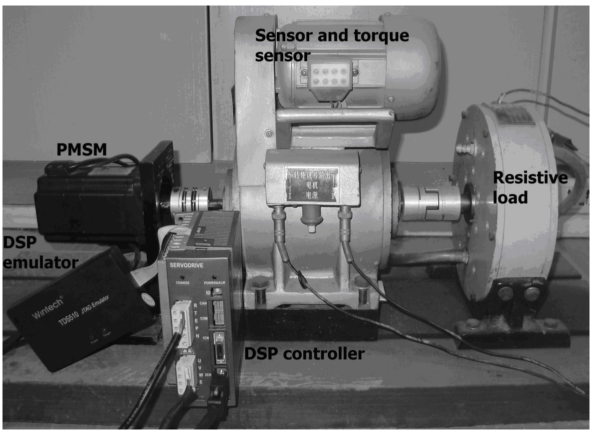

Fig. 3. Test bench.

Parameters	ITSM control	ASC
α_1	$\frac{1}{2}$	1
k_1	10	10
α_2	$\frac{2}{3}$	1
k_2	10	10
η	350	350
k_p	100	100
k_i	100	100
k	10	10

Tab. 2. Controller parameter values.

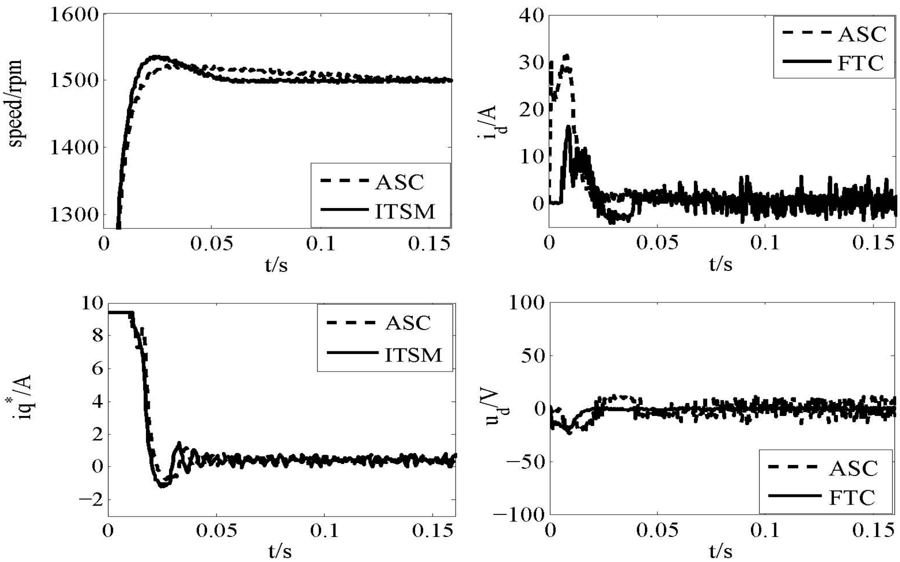

Fig. 4. The response curves when the reference speed value is 1500 rpm. (a) speed. (b) i_q^*. (c) i_d. (d) u_d.

4. CHATTERING ATTENUATION BASED ON A DISTURBANCE OBSERVER

From the Theorem 3.1, the integral terminal sliding mode control is naturally a kind of switching control, it adopts discontinuous switching gain term to suppress total disturbances, that is so say, the switching gain must be selected larger than the upper bound of the total disturbances. For practical application, due to conservative selective of the switching gain value η, we usually select too large, which may worse the system chattering phenomenon. Thus, if the disturbances can be well estimated and using feed-forward compensation, the switching gain η could be selected to be only larger than the upper bound of disturbance compensation error, then the system chattering phenomenon can be reduced.

4.1. Design of DOB-based composite controller

As we known, PMSM speed regulation systems always confront with different disturbances, including internal model uncertainties and external disturbances. Conventional feedback-based control methods usually can only reject these disturbances by feedback regulation indirectly in a relatively slow way. This results will degrade the PMSM system performance when meeting severe lump disturbances. One efficient way is to introduce a feed-forward compensation part into the conventional feedback controller for improving system performance, then a composite control scheme is designed. In most of real applications, it is usually impossible to measure the disturbances directly, so disturbance observation (DOB) techniques one of such efficient techniques which need to be devel-

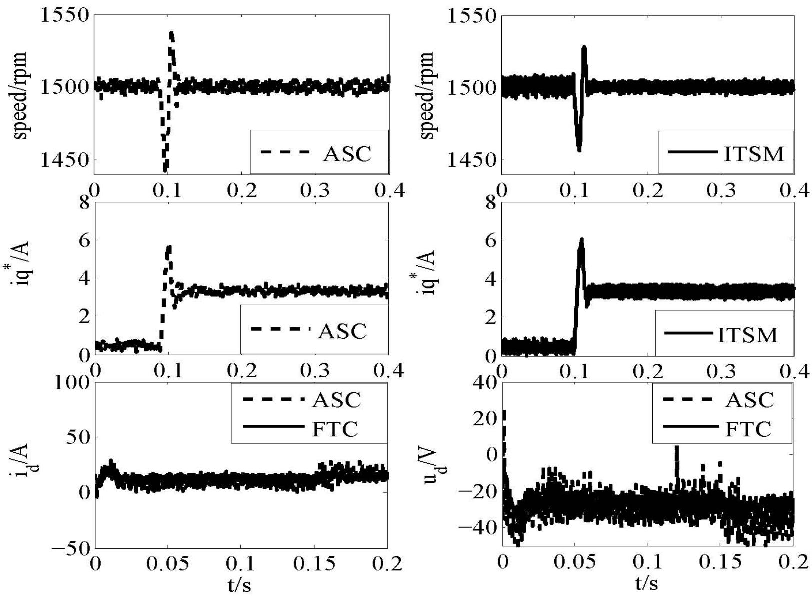

Fig. 5. The response curves when the reference speed value is 1500 rpm. (a) speed of ASC. (b) i_q^* of ASC. (c) speed of ITSM control. (d) i_q^* of ITSM control. (e) i_d. (f) u_d.

oped. The diagram of disturbance observer (DOB) based ITSM control system is shown as Figure 6.

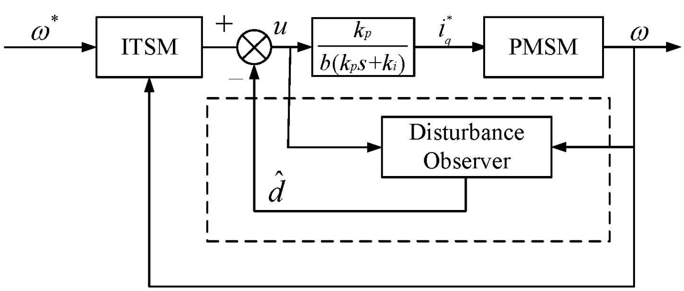

Fig. 6. Block diagram of DOB based ITSM control for PMSM system.

Definition 4.1: The disturbance estimation error $e_d(t)$ between the total disturbances $d(t)$ and the estimation is denoted as $e_d(t) = d(t) - \hat{d}(t)$.

Theorem 4.1: If the disturbance $d(t)$ satisfies Assumption 3.1, then the estimation error $e_d(t)$ will asymptotically approach to zero, the disturbance estimation $\hat{d}(t)$ will finally converge to the lumped disturbances $d(t)$. Considering system Eqs. (14) − (15), a disturbance observer is given as follows:

$$\begin{aligned} \hat{d}(t) &= \lambda(x_2 - z) \\ \dot{z} &= -u - \hat{d}(t) + \ddot{\omega}^* \end{aligned} \tag{32}$$

P r o o f. It can be obtained from Figure 6 that

$$e_d(t) = d(t) - \hat{d}(t). \tag{33}$$

Taking the derivation of Eq. (33), substitutes Eq. (32) in the Eq. (33), yields

$$\begin{aligned} \dot{e}_d(t) &= \dot{d}(t) - \dot{\hat{d}}(t) = \dot{d}(t) - \lambda(\dot{x}_2 - \dot{z}) && (34) \\ &= \dot{d}(t) - \lambda((-u - d(t) + \ddot{\omega}^*) - (-u - \hat{d}(t) + \ddot{\omega}^*)) && (35) \\ &= \dot{d}(t) - \lambda(d(t) - \hat{d}(t)) = \dot{d}(t) - \lambda e_d(t). && (36) \end{aligned}$$

According to the Lemma 5.5 in [12] (pp. 219), the system Eq. (43) is globally input-to-output (ISS). Combining $\lim_{t\to\infty} \dot{d}(t) = 0$ in Assumption 3.1, it is derived from the definition of ISS in [12] (pp. 217–218) that the state of system Eq. (43) converges to zero as $t \to \infty$, that is

$$\lim_{t\to\infty} e_d(t) \;=\; 0 \tag{37}$$

so the theorem 4.1 is thus proved.

The closed-loop system stability analysis here consists of the analysis for q-axis subsystem which adopts DOB based integral terminal sliding mode (ITSM) controller as.

$$\begin{aligned} u &= k_1 sig^{\alpha_1}(x_1(t)) + k_2 sig^{\alpha_2}(x_2(t)) + \eta sgn(s) + \ddot{\omega}^* - \hat{d}(t) \\ b(\dot{i}_q^* + \frac{k_i}{k_p} i_q^*) &= k_1 sig^{\alpha_1}(x_1(t)) + k_2 sig^{\alpha_2}(x_2(t)) + \eta sgn(s) + \ddot{\omega}^* - \hat{d}(t) \end{aligned} \tag{38}$$

where $\eta > l_e$, $k_1, k_2 > 0$, and α_1, α_2 satisfy $\alpha_2 = \frac{2\alpha_1}{1+\alpha_1}$ with $0 < \alpha_1 < 1$. □

Assumption 4.1: For the PMSM servo system, suppose there exists a constant $l_e > 0$, and it satisfies $|d(t) - \hat{d}(t)| \le l_e$.

Theorem 4.2: Suppose the PMSM servo system satisfies Assumption 4.1, the i_q^* control laws are designed as above Eqs. (24), if the switching gain satisfies $\eta > l_e$, then the closed-loop speed servo system of Eqs. (1) − (3) and (24) is globally finite-time stable.

P r o o f. For the second integrator system of Eqs. (20 − 21), choosing the following Lyapunov function

$$V = \frac{1}{2} s^T s \tag{39}$$

By taking the time derivative of V by using above Eq. (22), we obtain

$$\dot{V} = s\dot{s} = s(\dot{x}_2 + k_1 sig^{\alpha_1}(x_1) + k_2 sig^{\alpha_2}(x_2)) \tag{40}$$

then,

$$\begin{aligned}\dot{x}_2 &= u + d(t) = -k_1 sig^{\alpha_1}(x_1) - k_2 sig^{\alpha_2}(x_2) \\ &- \eta sgn(s) + \hat{d}(t) - d(t)\end{aligned} \tag{41}$$

substituting Eq. (41) into Eq. (40), it yields

$$\begin{aligned}\dot{V} &= s(-\eta sgn(s) - \hat{d}(t) + d(t)) \leq\mid s \mid (-\eta + l_e) \\ &= 2^{\frac{1}{2}}(-\eta + l_e)\left(\frac{1}{2}s^T s\right)^{\frac{1}{2}} = -2^{\frac{1}{2}}(\eta - l_e)V^{\frac{1}{2}}\end{aligned} \tag{42}$$

we know Eq. (42) satisfies Lemma 2.1, so the system state is stabilized to sliding mode surface in finite-time t_{q1} when $\eta > l_e \geq |d(t) - \hat{d}(t)|$.

From the above analysis, the system states will reach the sliding surface $s = 0$ from any initial condition in finite-time t_{q1}, then $\dot{s} = 0$, yields

$$\dot{s} = \dot{x}_2 + k_1 sig^{\alpha_1}(x_1) + k_2 sig^{\alpha_2}(x_2) = 0 \tag{43}$$

According to Lemma 2.2, we know that the system state can converge to the origin along the sliding surface in finite-time t_{q2} . This completes the proof of q-axis closed-loop subsystem stability. The proof of d-axis closed-loop subsystem stability is the same as the last part. So this completes the proof. □

Remark 3.1: The observer convergence is tuned by the value λ, it could be choosed as large as possible, then the observer convergence is fast. The observer convergence rate could be faster than controller, but overlarge value may lead in much noise. Due to the disturbance estimation based feed-forward compensation, the switching gain η only need to be larger than observer error bound "l_e", thus the chattering phenomenon is reduced.

4.2. Experimental results

This PMSM system under these two control schemes, ITSM control method and ITSM+DOB method, it use the same test bench. The experiment parameter is selected as following Table 3.

The experiment results of speed response are shown in Figure 7(a) and Figure 7(b), experiment result in Figure 7(a) show that the method of ITSM+DOB control and finite control method give a shorter settling time with smaller overshoot as compared with ITSM control method. Figure 8(a), and Figure 8(c) show that the ITSM+DOB control method has less fluctuation and a shorter recovering time compared with the ITSM control method, the speed drop of ITSM+DOB method is 45 rpm, ITSM control method has 29 rpm with speed drop. From Figure 7(b), Figure 8(b), and Figure 8(d),

Parameters	ITSM+DOB control	ITSM control
α_1	$\frac{1}{2}$	$\frac{1}{2}$
k_1	10	10
α_2	$\frac{2}{3}$	$\frac{2}{3}$
k_2	10	10
η	350	150
k_p	100	100
k_i	100	100
k	0.05	0.05
$\frac{1}{\lambda} = \frac{1}{\tau}$	200	–

Tab. 3. Controller parameter values.

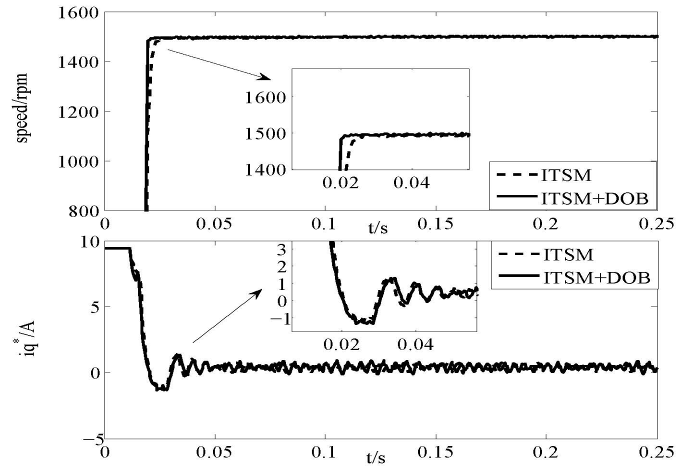

Fig. 7. The response curves when the reference speed value is 1500 rpm. (a) speed. (b) i_q^*.

the response of i_q^* recovers faster than the current response of ITSM both at the initial time and when the load torque disturbance is given suddenly. Notice that the chattering phenomenon is obvious reduced based on the disturbance compensation, the disturbance rejection is also enhanced.

5. CONCLUSION

In this paper, the design and implementation of q-axis speed controller and d-axis current controller using integral terminal sliding mode control and finite-time control based on feedback-linearization technique have been given. The rigorous analysis for the closed loop system has shown that the system state could be stabilized and track the reference signal in finite time. Compared with the asymptotically stable controller, the proposed

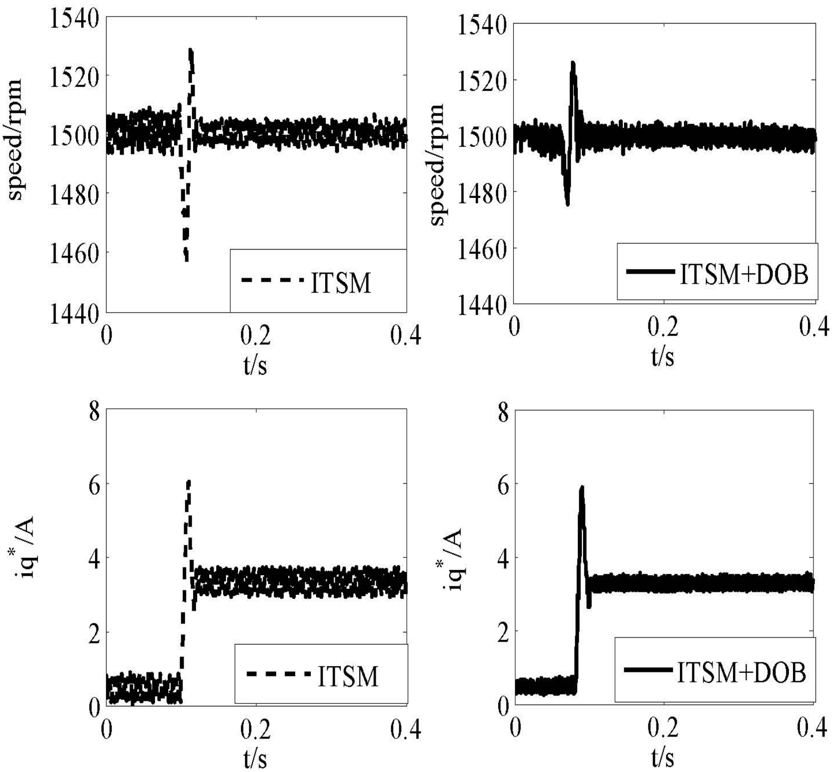

Fig. 8. The response curves when in the presence of disturbance. (a) speed of ITSM control. (b) i_q^* of ITSM control. (c) speed of ITSM+DOB. (d) i_q^* of ITSM+DOB.

control scheme not only ensure the stability of closed loop system, but also make the convergence rate and the disturbance reject performance much better. For reducing chattering phenomenon, the disturbance compensation technique has been introduced. Finally, the effectiveness of proposed method has been verified by experimental results.

ACKNOWLEDGEMENT

This work was supported in part by National Natural Science Foundation (NNSF) of China under Grants (61803335) and (51877207), and NSFC-Zhejiang Joint Fund for the Integration of Industrialization and Informatization (U1709213).

(Received December 27, 2017)

REFERENCES

[1] S. P. Bhat and D. S. Bernstein: Finite-time stability of homogeneous systems. In: Proc. American Control Conference, Albuquerque 1997, pp. 2513–2516. DOI:10.1109/acc.1997.609245

[2] S. P. Bhat and D. S. Bernstein: Finite-time stability of continuous autonomous systems. SIAM J. Control Optim. *38* (1998), 751–766. DOI:10.1137/s0363012997321358

[3] S. P. Bhat and D. S. Bernstein: Continuous finite-time stabilization of the translational and rotational double integrators. IEEE Trans. Automat. Control *43* (1998), 678–682. DOI:10.1109/9.668834

[4] S. P. Bhat and D. S. Bernstein: Geometric homogeneity with applications to finite time stability. Math. Control Signals System *17* (2005), 101–127. DOI:10.1007/s00498-005-0151-x

[5] W. H. Chen: Disturbance observer based control for nonlinear systems. IEEE ASME Trans. Mechatron. *9*(2004), 4, 706–710. DOI:10.1109/tmech.2004.839034

[6] T. L. Chern and Y. C. Wu: An optimal variable structure control with integral compensation for electrohydraulic position servo control systems. IEEE Trans. Ind. Electron. *39* (1992), 5, 460–463. DOI:10.1109/41.161478

[7] Y. Feng, J. F. Zheng, X. H. Yu, and Nguyen Vu: High-order terminal sliding-mode observer design method for a permanent-magnet. synchronous motor control system. IEEE Trans. Ind. Electron. *56* (2009), 9, 3424–3431. DOI:10.1109/tie.2009.2025290

[8] L. Guo and W. H. Chen: Disturbance attenuation and rejection for systems with nonlinearity via DOBC approach. Int. J. Robust Nonlinear Control *15* (2005), 3, 109–125. DOI:10.1002/rnc.978

[9] V. T. Haimo: Finite-time controllers. SIAM J. Control Optim. *24* (1986), 760–770. DOI:10.1137/0324047

[10] J. Han: From PID to active disturbance rejection control. IEEE Trans. Ind. Electron. *56* (2009), 3, 900–906. DOI:10.1109/tie.2008.2011621

[11] T. L. Hsien, Y. Y. Sun, and M. C. Tai: H1 control for a sensorless permanent-magnet Synchronous drive. IEE Proc. Electr. Power. Appl. *144* (1997), 3, 173–181. DOI:10.1049/ip-epa:19970988

[12] H. K. Khail: Nonlinear Systems PID predictive controller. Third Edition. Upper Saddle River, Prentice-Hall, NJ 1996.

[13] H. Kim, J. Son, and J. Lee: A high-speed sliding-mode observer for the sensorless speed control of a PMSM. IEEE Trans. Ind. Electron. *58* (2011), 9, 4069–4077. DOI:10.1109/tie.2010.2098357

[14] Y. S. Kung and M. H. Tsai: FPGA-based speed control IC for PMSM drive with adaptive fuzzy control. IEEE Trans. Power. Electron. *22* (2007), 6, 2476–2486. DOI:10.1109/tpel.2007.909185

[15] C. K. Lai and K. K. Shyu: A novel motor drive Design for incremental motion system via sliding-mode control method. IEEE Trans. Ind. Electron. *52* (2005), 2, 499–507. DOI:10.1109/tie.2005.844230

[16] V. Q. Leu, J. C. Han, and J. W. Jung: Fuzzy sliding mode speed controller for PM synchronous motors with a load torque observer. IEEE Trans. Pow. Electron. *27* (2012), 3, 1530–1539. DOI:10.1109/tpel.2011.2161488

[17] A. Levant: Robust exact differentiation via sliding mode technique. Automatica *34* (1998), 3, 379–384. DOI:10.1016/s0005-1098(97)00209-4

[18] J. Li, S. H. Li, and X. S. Chen: Adaptive speed control of PMSM servo system using a RBFN disturbance observer. Trans. Inst. Meas. Control *34* (2012), 5, 615–626. DOI:10.1177/0142331211410920

[19] S. H. Li and Z. G. Liu: A daptive speed control for permanent-magnet synchronous motor system with variations of load inertia. IEEE Trans. Ind. Electron. *56* (2009), 8, 3050–3059. DOI:10.1109/tie.2009.2024655

[20] S. H. Li, H. X. Liu, and S. H. Ding: A speed control for a PMSM using finite-time feedback control and disturbance compensation. Trans. Inst. Meas. Control. *32* (2010), 2, 170–187. DOI:10.1177/0142331209339860

[21] S. H. Li and Y. P. Tian: Finite-time stability of cascaded time-varying systems. Int. J. Control *80* (2007), 4, 646–657. DOI:10.1080/00207170601148291

[22] S. H. Li, K. Zong, and H. X. Liu: A composite speed controller based on a second-order model of permanent magnet synchronous motor system. Trans. Inst. Meas. Control. *33* (2011), 5, 522–541. DOI:10.1177/0142331210371814

[23] S. H. Li, M. M. Zhou, and X. H. Yu: Design and implementation of terminal sliding mode control method for PMSM speed regulation system. IEEE Trans. Ind. Inform. *9* (2013), 4, 1879–1891. DOI:10.1109/tii.2012.2226896

[24] Y. Luo, Y. Q. Chen, H. S. Ahnc, and Y. Pi: Fractional order robust control for cogging effect compensation in PMSM position servo systems: stability analysis and experiments. Control. Eng. Practice. *18* (2010), 9, 1022–1036. DOI:10.1016/j.conengprac.2010.05.005

[25] J. H. She, M. Y. Fang, H. Ohyama, H. Hashimoto, and M. Wu: Improving disturbance-rejection performance based on an equivalent-input-disturbance approach. IEEE Trans. Ind. Electron. *55* (2008), 1, 380–389. DOI:10.1109/tie.2007.905976

[26] R. Y. Tang: Modern permanent magnet synchronous motor theory and design. Machinery Industry Press, Beijing 1997.

[27] T. Umeno, and Y. Hori: Robust speed control of DC servo motors using modern two degrees-of-freedom controller design. IEEE Trans. Ind. Electron. *38* (1991), 5, 363–368. DOI:10.1109/41.97556

[28] G. Vilath, M. Rahman, K. Tseng, and M. Uddin: Nonlinear control of interior permanent magnet synchronous motor. IEEE Trans. Indust. Appl. *39* (2003), 2, 408–415. DOI:10.1109/tia.2003.808932

[29] G. J. Wang, C. T. Fong, and K. J. Chang: Neural-network-based self-tuning PI controller for precise motion control of PMAC motors. IEEE Trans. Ind. Electron. *48* (2001), 2, 408–415. DOI:10.1109/41.915420

[30] J. Wang, F. Wang, G. Wang, et al.: Generalized proportional integral observer-based robust finite control set predictive current control for induction motor systems with time-varying disturbances. IEEE Trans. Ind. Informa. *14* (2018), 9, 4159–4168. DOI:10.1109/tii.2018.2818153

[31] J. Wang, F. Wang, Z. Zhang, et al.: Design and implementation of disturbance compensation-based enhanced robust finite control set predictive torque control for induction motor systems. IEEE Trans. Ind. Inforn. *13* (2017), 5, 2645–2656. DOI:10.1109/tii.2017.2679283

[32] J. Yang, S. H. Li, and X. H. Yu: Sliding mode control for systems with mismatched uncertainties via a disturbance observer. IEEE Trans. Ind. Electron. *60* (2013), 1, 160–169. DOI:10.1109/tie.2012.2183841

[33] J. Yang, H. Wu, L. Hu, et al.: Robust predictive speed regulation of converter-driven DC Motors via a discrete-time reduced-order GPIO. IEEE Trans. Ind. Electron, online (2018).

[34] H. A. Zarchi, G. R. A. Markadeh, and J. Soltani: Direct torque and flux regulation of synchronous reluctance motor drives based on input-output feedback linearization. Energy. Convers. Manag. *51* (2010), 1, 71–80. DOI:10.1016/j.enconman.2009.08.031

[35] J. Zhou and Y. Wang: Adaptive backstepping speed controller design for a Permanent magnet synchronous motor. IEE Proc. Electr. Power. Appl. *149* (2002), 2, 165–72. DOI:10.1049/ip-epa:20020187

[36] Q. Zong, Z. S. Zhao, and J. Zhang: Higher order sliding mode control with self-tuning law based on integral sliding mode. IET Contr. Theory. Appl. *4* (2010), 7, 1282–1289. DOI:10.1049/iet-cta.2008.0610

Junxiao Wang, College of Information Engineering, Zhejiang University of Technology, Hangzhou, 310023, China, and also with the Key Laboratory of Industrial Internet of Things and Networked Control, Ministry of Education, Chongqing University of Posts and Telecommunications, Chongqing, 400065. P. R. China.
e-mail: wangjunxiao19860128@126.com, wjx2017@zjut.edu.cn

Fengxiang Wang, Quanzhou Institute of Equipment Manufacturing, Haixi Institutes, Chinese Academy of Sciences, Jinjiang. P. R. China.
e-mail: fengxiang.wang@fjirsm.ac.cn

Xianbo Wang, College of Electrical Engineering, Henan University of Technology, Zhengzhou, 450001, China
e-mail: xb_wang@live.com

Li Yu, College of Information Engineering, Zhejiang University of Technology, Hangzhou, 310023. P. R. China.
e-mail: lyu@zjut.edu.cn